SUB-DAILY EARTH ROTATION DURING EPOCH '92

A. P. FREEDMAN, R. IBANEZ-MEIER, J. O. DICKEY, S. M. LICHTEN
Jet Propulsion Laboratory
California Institute of Technology
Pasadena, California 91109

T. A. HERRING
Department of Earth, Atmospheric, and Planetary Sciences
Massachusetts Institute of Technology
Cambridge, Massachusetts 02139

ABSTRACT. Earth rotation data were obtained with GPS during the Epoch '92 campaign in the summer of 1992. About 10 days of data were acquired from 25 globally distributed stations and a constellation of 17 GPS satellites. These data were processed to estimate UT1 corrections every 30-minutes, then smoothed to form a UT1 series with 3-hour spacing. Earth orientation data during Epoch '92 were also obtained by several VLBI groups, and were processed together to yield VLBI estimates of UT1 with 3-hour time resolution. The high frequency behavior of both GPS and VLBI data sets is similar, although drifts between the two series of ~0.1 ms over 2-5 days are evident. Tidally induced UT1 variations from both theoretical ocean models and empirical determinations were compared with the GPS and VLBI series. Estimates of atmospheric angular momentum (AAM) at 6 hour intervals generated by several meteorological centers were also compared with the geodetic data. These comparisons indicate that most of the GPS signal in the diurnal and semidiurnal bands can be attributed to tidal processes, and that UT1 variations over a few days are mostly atmospheric in origin.

Introduction

Variations in the rate of rotation of the solid Earth result both from torques applied to the Earth from the exterior or interior and from mass redistributions within the Earth. For high-frequency (sub-daily) rotation variations, defined here as rotation rate changes occurring over time scales of a week or less, the principal forces on the solid Earth are thought to come from the atmosphere and oceans. In particular, tidal forcing of the oceans is expected to dominate the rotational variations at periods of one day and less.

A variety of techniques have historically been used to monitor the rotation of the Earth, but only over the past few years has the capability for daily and even sub-daily monitoring of Earth rotation with the requisite precision become available. Current high-precision techniques include very long baseline interferometry (VLBI), satellite laser ranging (SLR), lunar laser ranging (LLR), and, most recently, the Global Positioning System (GPS). VLBI estimates of Earth's rotation angle (UT1-UTC) at daily intervals and SLR estimates at roughly 3-day intervals have been made for several years. Over the past four years, measurements of UT1 variations with hourly or so time resolution have been made sporadically by both VLBI and GPS techniques [1, 2].

In association with the International GPS Geodynamics Service's (IGS) proof of concept campaign for the summer of 199?, an additional campaign known as SEARCH '92 (Study of Earth-Atmosphere Rapid Changes) was held to monitor high-frequency Earth orientation variations utilizing all space geodetic techniques and to advocate for and facilitate the collection of the best available related geophysical data [3]. Data from a variety of complementary techniques providing a good level of redundancy were acquired, in particular, during the intensive. two-week period known as Epoch '92. In this paper, we present GPS estimates of sub-daily variations in UT1 during Epoch '92 and compare these results with a number of these ohm related data sets, This intercomparison should provide a robust estimate of Earth's true rotational variations at time scales as short as a few hours, and should help as well to improve strategies for processing GPS data.

2. Data sets

2.1. GPS

The GPS data processing strategy is a version of that discussed elsewhere using the JPL GIPSY/OASIS II software [4, 5] and is summarized in Table 1 [see also Zumberge et al., this volume]. Data from a network of 25 stations using a GPS constellation of 17 satellites were acquired over more than 10 days during the last week of July and first week of August, 1992. Owing to the use of anti-spoofing (AS) signal encryption over the weekend, these data are not continuous but are divided into two groups from which two multi-day GPS orbit arcs were created. Corrections to a nominal UTPM series (derived from the IERS Bulletin B) were obtained from the data, with UT1 estimated every 30 minutes and polar motion every two hours. UT1 was modeled as a Gauss-Markov (AR1) process with a steady-state sigma of 0.06 ms and a time constant of 4 hours. Thus, over 30 minutes, 0.028 ms of process noise was added.

Table 1. GPS ESTIMATION STRATEGY

Estimated parameters	
Station locations (8 fiducial sites)	Wet zenith troposphere (random walk)
Satellite states	Clock biases (white-noise)
Solar radiation pressure	Carrier phase biases
UT1 (AR1)	Polar motion (white noise)
Standard Models	
Solid Earth tides and equilibrium ocean tides from Yoder et al. [6]	
Gravity field coefficients: GEM-T3, 8x8 truncation	
Nutation model: 1980 IAU model	
A priori and fiducial site locations ITRF91	
Nominal UTPM from IERS Bulletin B	
Rogue receivers: Pseudorange (1-meter), Carrier Phase (1 cm)	
6-minute data interval (obtained by decimation)	

We generated UT1 time series using a variety of orbit modeling strategies [Zumberge et al., this volume]. Our preferred strategy employed multi-day orbit arcs wherein one set of satellite states (positions and velocities) was estimated for each satellite. Three stochastic solar radiation parameters for each satellite were modeled as AR1 processes and estimated every hour. Alternative estimation strategies yield UT1 series that differ, but the results and conclusions described below do not significantly change if these other UT1 series are used.

For comparison with the VLBI data, we constructed a smoothed GPS UT1 data set by applying a Gaussian filter with a half-width of about one-half hour to smooth the 30-minute data and inter-

polate them to the epochs of the VLBI data. Although it contains GPS-derived UT1 measurements every 3 hours, this smoothed data set is not identical to a 3-hour GPS solution, since the latter contains UT1 values averaged over a 3-hour window whereas the former is effectively smoothed over a 1- to 2-hour window.

2.2. VLBI

VLBI data were acquired from the three networks described in Table 2. Note that on certain days, UT1 was measured by more than one VLBI network, enabling an estimate of the quality of the VLBI data. The correlated VLBI data were combined using the MIT Kalman filter programs CALC/SOLVK. UT1, polar motion, nutation corrections, and station troposphere parameters were estimated over 24 hour time spans, with UT1, polar motion, and the troposphere parameters modeled as random walks [see Herring, this volume].

Several solutions were generated in which UT1 was estimated either every 30 minutes or every 3 hours. The 30-minute solutions were rather noisy, so a 3-hour series, in which UT1 was estimated every 3 hours with 0.04 ms sigma resets after a diurnal and semidiurnal a priori tide model had been applied, was used in this study. A final smoothed VLBI solution was generated in which the 24-hour data sets from all the networks were combined using a mild Gaussian filter.

Table 2. VLBI DATA

NASA's Goddard Space Flight Center (GSFC) - NASA R&D
8 experiments, 5-6 sites in N. America, Hawaii, and Europe
National Oceanic and Atmospheric Administration's (NOAA) Laboratory for Geosciences - IRIS
4 experiments (oat mobile, three IRIS SA), 5 sites in N. America and 1 Europe
Unites States Naval Observatory (USNO) - NAVNET
6 experiments, 4-6 sites, located around globe
Data run from July 26 through August 11. Four days have measurements by both NAVNET and NASA R&D. Each experiment can have significantly different formal errors.

2.3. TIDE MODELS

A variety of additional data sets were used in evaluating the GPS and VLBI time series. Two models for tidally-induced diurnal and semidiurnal UT1 variations were compared, one based on theoretical ocean models [7] and oat. empirically derived from many years of measured UT variations [8]. The theoretical series, referred to as the Gross tick model, is based on the oceanic angular momentum model of Seiler [9]. This formulation also contains corrections to the standard tide model [6] for non-equilibrium ocean tides at fortnightly and monthly periods. The empirical model, referred to as the Herring tide model, is based on 8 years of VLBI data. It contains estimates of the dismal and semidiurnal tidal terms only. Note. that this empirical tide. series may contain additional diurnal signals other than those due to the non-equilibrium ocean tides, such as the effects of atmospheric tides. Both tidal UT1 series may be compared directly to geodetic UT1 estimates.

2.4. AAM GUIDANCE DATA

If angular momentum were exchanged solely between the atmosphere and the solid Earth, atmospheric angular momentum (AAM) variations would result in corresponding changes in the length of the day (LOD), the time derivative of UT1. Several sets of AAM were computed every 6 hours as part of the SEARCH/IGS effort by three meteorological centers: the U. S. National

Meteorological Center (NMC), the European Centre for Medium-Range Weather Forecasts (ECMWF), and the Japanese Meteorological Agency (JMA). For each center, the AAM quantity that we use consists of the χ_3 AAM wind term integrated to the top of the model atmosphere (either 50 mbar or 10 mbar, depending on center) plus the fall pressure (not inverted-barometer) term. Gaps in the AAM series were filled by linear interpolation.

We used these data sets to estimate atmospherically induced variations in UT1. Since AAM is a substitute LOD, the AAM series must be integrated to be compared to a UT1 series. However, two arbitrary constants, effectively a bias in LOD and a bias in UT1, enter into this integration. For the comparisons shown below, linear models are removed from the AAM and geodetic UT1 series to account for these constants.

2.5. SMOOTHED REFERENCE SERIES

A reference series, based on the IERS Bulletin B nominal values used for the GPS analysis, was used to remove long-period UT1 variations. Note that all the geodetic series shown have the shorter-period (<35 day) tides explicitly removed according to the standard Yoder et al. [6] model, while subtracting the nominal UT1R series effectively removes the longer period terms of [6].

3. Results

3.1. GPS *vs.* VLBI

We have compared the GPS-derived UT1 with VLBI estimates of UT1-TAI for each network-day of data. UT1 was estimated every 30 minutes in both sets of data. Typical formal errors of the various time series are summarized in Table 3. We present below only results for the smoothed and interpolated sets of VLBI and GPS data. These two data sets are shown in Figure 1. For display purposes, the UT1 values have been differenced with the IERS Bulletin B reference series. The bias between GPS and VLBI is arbitrary. Note the gap in GPS data due to the use of AS during the weekend of August 1-2 which precludes the construction of a continuous two-week long GPS time series. The 6-day time span at the end of July where data exist from both techniques is referred to below as period A, while the 4.5-day time span in August is referred to as period B.

Although there appears to be a drift between the two series over several days, their diurnal variability is similar. If the two series are differenced, linear trends can be fit separately to periods A and B to quantify both the drift and residual scatter in GPS minus VLBI. These values are given in Table 3. Over 4106 day time spans, the GPS shows a fairly linear drift with respect to VLBI, with drift rates of $\pm$20-40 μsec/day. After removing these drifts, the total RMS scatter of GPS minus VLBI UT1 is 0.023 ms. These drifts are probably a result of drift in the GPS time series caused by systematic effects such as orbit mismodeling.

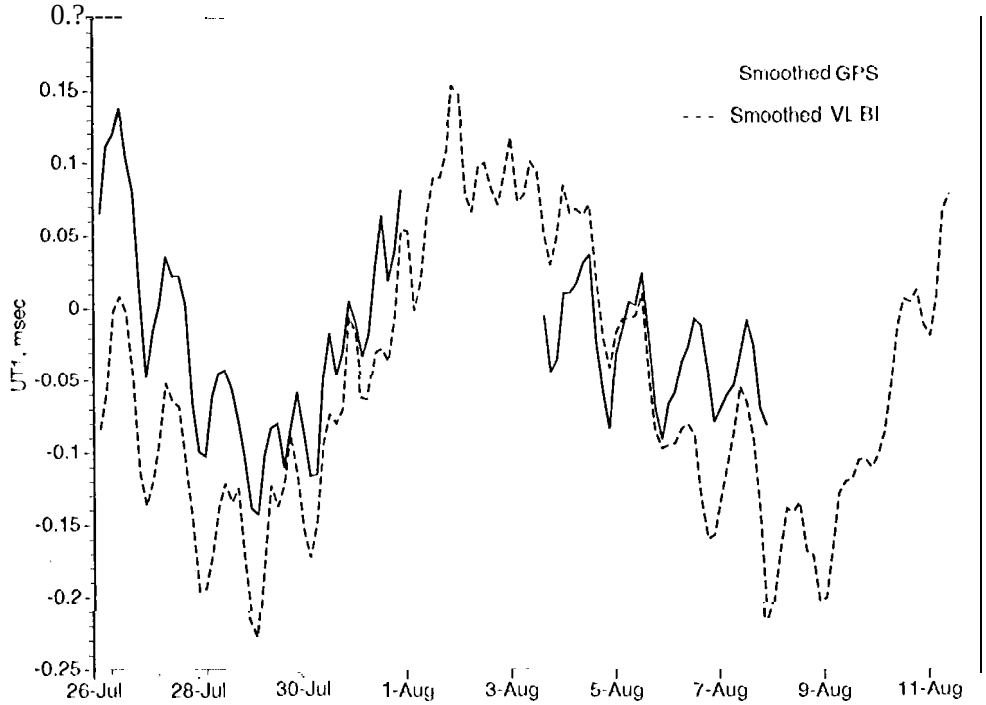

Fig. 1. UT1 from GPS and VLBI evaluated every 3 hours.

Table 3. STATISTICS

	Typical 30-Minute UT1 Formal Errors		
GPS	**IRIS VLBI**	**NAVNET**	NASA **R&D**
0.0? -().()3 ms	0.02-().()4 ms	0.015 -().()-1 Ins	0.01 -0.025 ms
	GPS Minus VLBI		
	Period A	**J'cried B**	**Entire time span**
Slope	-().()1 8ms/day	0.041 ms/day	
RMS scatter	0.022 ms	0.026 ms	0.023 ms
	GPSMinus '1'ides		
	GPS UT1 only	**GPS minus Herring**	**GPS minus Grins**
RMS Scatter	0.032 ms	*0.018* ms	*0.035* ms
	UT1 Minus (AA M-t 'J'ides)		
RMS of difference	**NMC** AAM	**ECMWF AAM**	**JMA** AAM
GPS UT1	**0.0?** 1 ms	0.()?? ms	0.019 ms
VLBI UT1	0.()?7 ms	0.022 ms	0.022 ms

The relationship between GPS and VLBI may be further explored by computing power spectra of the GPS and VI .13111'1'1 and their difference (Fig. 2). Power spectra were obtained separately for the two periods A and B (after padding with zeros to the same length) and averaged together. A 3-point spectral smoothing was used (corresponding to a bin width of 0.375 cycles per day). Both the VI .BI and GPS series show similar power in the diurnal and semidiurnal bands. Differencing the two removes the. peaks in power at both frequencies, suggesting that there is a true geodetic signal in these binds that is accurately sensed by both techniques. This signal is for the most part tidal in origin, as shown I3c1ow.

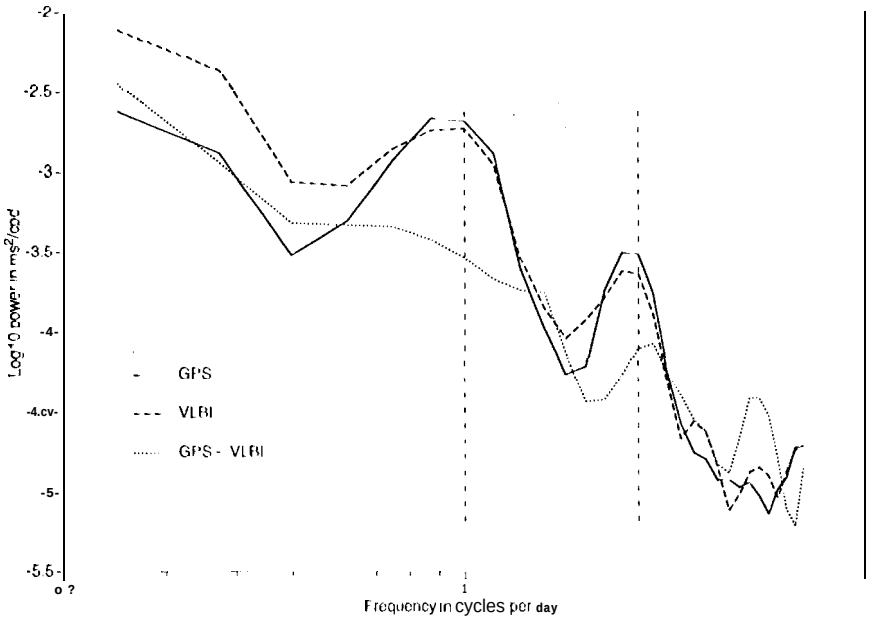

Fig. 2. Power spectra of theGPSandVLBIUT1 series and their difference.

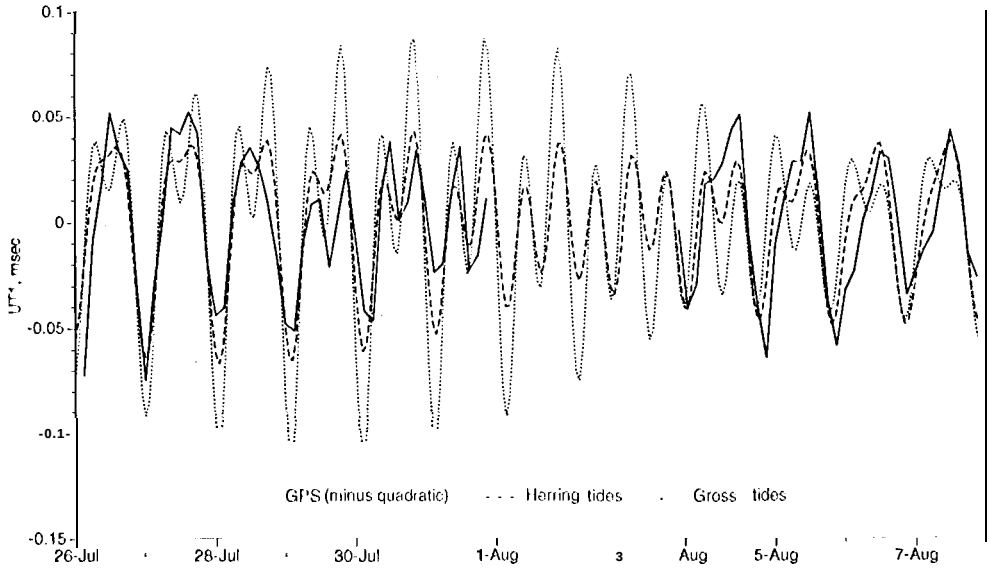

Fig. 3. GPSUT1 compared to two models of tidally induced UT1 variations.

3.2. GPS VS. TIDES

In Figure 3, we compare the smoothed GPS UT1 to the two models of tidally -induced UT1 variations. The GPS series for each period (A and B) has had a best-fitting quadratic subtracted to remove longer-period fluctuations, thus making the residual series easy to compare with the tides. Note that the Herring, empirical model more accurately reflects the observed UT1 variability than does the Gross, theoretical model.

These differences can again be described through the use of power spectra. Power spectra (computed as before) of the GPS UT1 series and the GPS series minus the two tide models are shown in Fig. 4. The Herring model removes most of the excess power in the diurnal and semidiurnal bands, with a hint of signal remaining at *2 cycles* per day (cpd). The Gross model removes some power at diurnal frequencies, but adds substantial power at semidiurnal frequencies (consistent with the large amplitudes seen in Fig. 3). These differences are quantified in Table 3, which shows the RMS scatter of the three time. series whose power spectra are plotted in Fig. 4. The Herring model appears to more accurately reflect the actual UT1 variations at diurnal and semidiurnal frequencies. Reasons for this may include inaccuracies in the theoretical ocean models and additional non-oceanic signal at these frequencies.

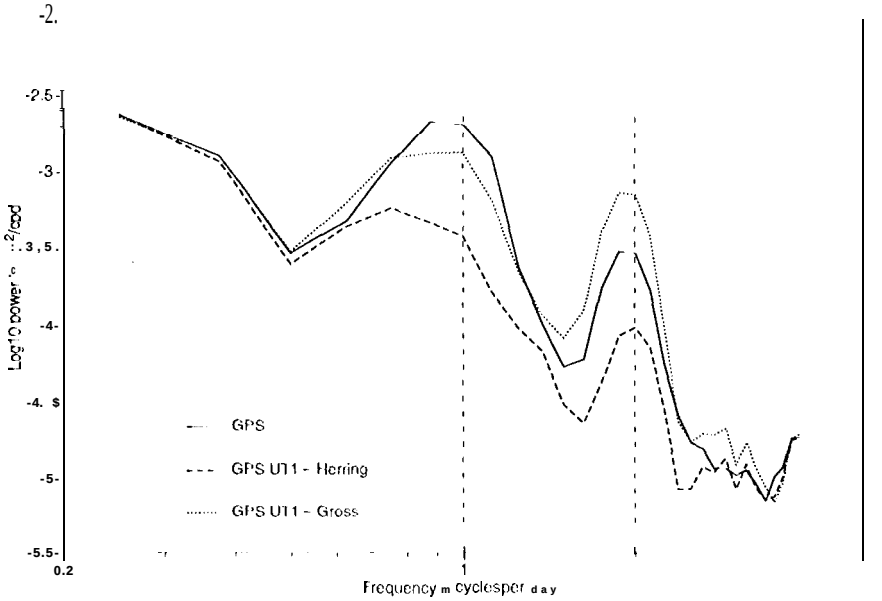

Fig. 4. Power spectra of the GPS UT1 series and the GPS series differenced with each of the two tide models.

3.3. GPS vs. AAM

The three series of atmospheric angular momentum (AAM) values evaluated every 6 hours provided by the NMC, the ECMWF, and the JMA are shown in Fig. 5. The variations in each series over periods greater than 1 to *2* days are similar, but the. higher frequency fluctuations do not appear to be common among the three. The biases between the series are real, and come from differences in the meteorological models of the centers.

Since A AM represents a form of LOD, the curves in Fig. 5 mast be numerically integrated to generate. UT1 series whose variations are implied by the AAM. These series are shows in Figure 6. Also shown arc a GPS UT1 series and the UT1 variations expected from the longer-period (J 4 and 30-day) non-equilibrium ocean ticks emerging from the. numerical ocean model [7]. 1 Each series for each of periods A and B has had a best-fitliag linear bias and trend removed. Since the ECMWF series for period A starts cm July 27 and thus is one clay shorter, it has had a trend removed which minimizes the cliffcre.aces between the 1 ECMWF curve and the other two A AM carves. The three integrated AAM carves show similar behavior for period A, with more coatras[-

ing forms for period B. All the AAM curves appear consistent with the overall shape of the GPS UT1 curve. The longer-period tick corrections do not add substantial signal at these few-day periods.

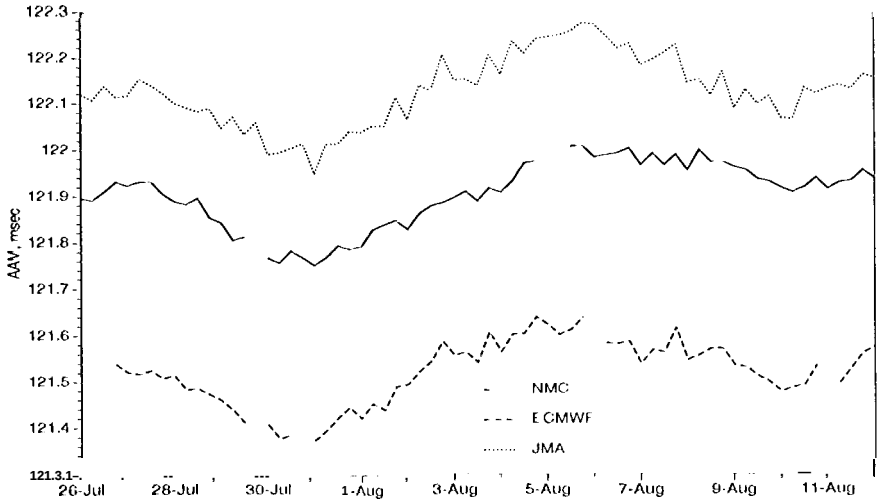

Fig. S. Three series of atmospheric angular momentum (AAM) values.

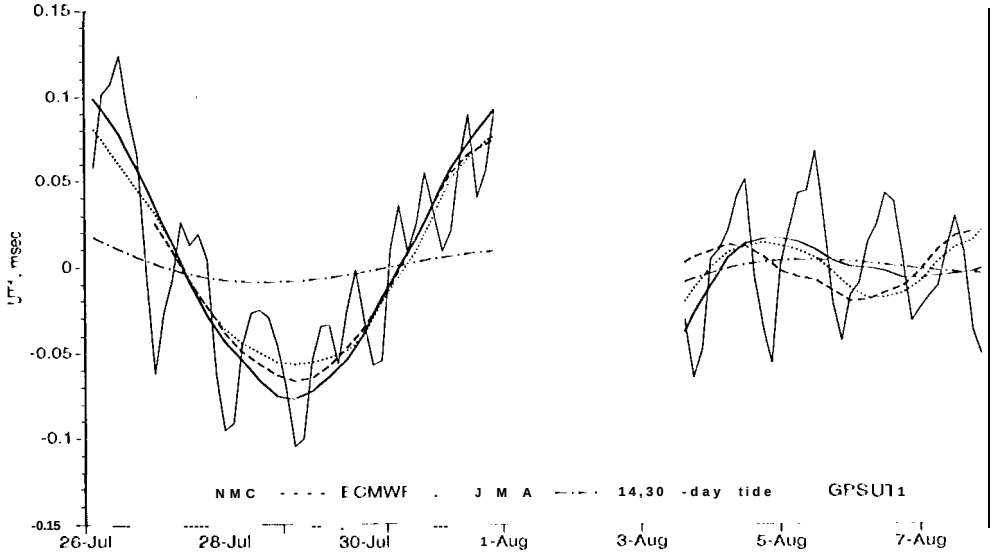

Fig. 6. Comparison of integrated AAM with geodetic UT1 variations.

The sum total of the integrated AAM, diurnal anti semidiurnal tides (from [8]) and longer-period tides (from [7]) are shown in Figure 7, together with the observed UT1 variations from GPS and VLBI. Linear trends were removed from each series for each period. Most of the geodetic signal can be described by the sum of AAM variations and tidally induced UT1, with the tides acting at periods of one day and less and AAM acting at periods greater than a day. The differences between GPS and VLBI are at least as large as those between the AAM series themselves and the AAM and geodetic series. Thus, no center or technique stands out as superior. The RMS

of the differences between the. geodetic and AAM+ tides series arc shown in Table 3; all are consistent with the typical GPS and VI .BI formal errors of ().02-().03 ms.

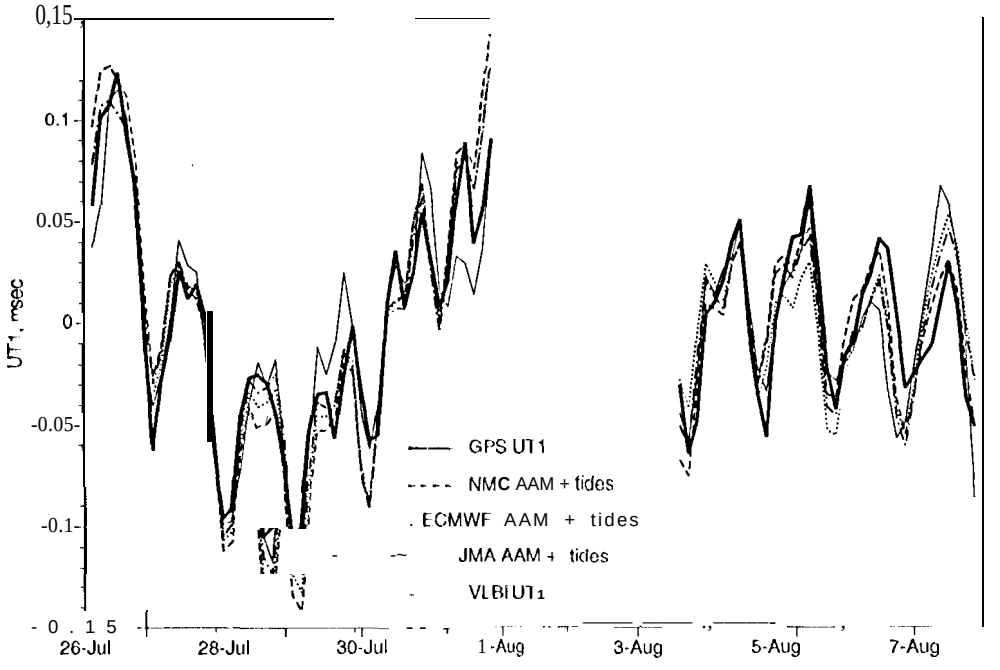

Fig. 7. The sum of the integrated AAM and diurnal, semidiurnal, and longer-period tides compared with the observed UT1 variations from GPS and VLBI.

4_0 Conclusions

Differences bet ween the various series considered here. tend to be at the. level of ().()2 to ().()3 ms. These RMS differences are consistent with the formal uncertainties of the data themselves. The main exception is the the.cwctical lick model, which simply does not yield the signal seen geodetitally. l'here is also a drift in the GPS data relative to VI .BI which, over time spans of 6 days or so, appears to be linear but with a non-unique drift MC..

Both GPS and VI .BI exhibit nearly identical variability y in the diurnal and semidiurnal bands, attributable to tidal variations whose value.s are well derived from many years of geodetic VI .BI data. '1'here is no residual signal in these frequency bands that C. xceeds the level of formal error of the data, although residual signals with amplitudes smaller than (),()2 ms could certainly be present. Although the theoretical tide. model does not agree with observations in either band, the disagreement is largest in the semidiurnal frequency band.

The multi-day variability of AAM from all the meteorological centers is similar, and yields AAM-derive.d UT1 curves that arc consistent with the variability of the geodetic UT1 at periods longer than one clay. At diurnal and shorter periods, however, the AAM centers generate inconsistent estimates. Moreover, the sub-daily variability of the AAM is quite small and cannot, at this point, be disentangled from oceanic tidal effects and noise in the geodetic data, However, limits can be placed cm the size of any residual AAM signal.

Thus the signal seen in the GPS time series can be represented by the sum of four effects: tides at diurnal and semi-diurnal periods, AAM fluctuations at periods of one to at least several days, a

linear drift in UT1 due possibly to orbit mismodeling, and a high-frequency mist component. To accurately solve for UT1 with GPS at these frequencies, the tidal variations in UT1 must certainly be modeled, either by explicit use of the Herring tide model, or by allowing, adequate variability in the estimated UT1. AAM-induced variations are slow enough that if UT1 (or LOD) is estimated at least daily, this variability need not be explicitly modeled. Further research is necessary to investigate and reduce both the drift in UT1 of -0.1 ms over 2-5 days, and the level of high-frequency noise present in the data.

ACKNOWLEDGMENTS. The authors thank and acknowledge the cast of literally thousands who were involved in collecting and processing the vast quantities of data from both GPS and VLBI, as well as the people and institutions involved in generating the AAM data sets. The work described in this paper was carried out by the Jet Propulsion Laboratory, California Institute of Technology, under contract with the National Aeronautics and Space Administration.

References

[1] Herring, T. A., and D. Dong, "Current and Future Accuracy of Earth Rotation Measurements," in *Proceedings of the AGU Chapman Conference on Geodetic VLBI: Monitoring Global Change (Washington DC, April 22-26, 1991) pp. 306-324,* NOAA Technical Report NOS 137 NGS 49, NOS/NOAA, Rockville, Ml), 1991.

[2] Lichten, S. M., S. L. Marcus, and J. O. Dickey, "Sub-Daily Resolution of Earth Relation Variations With Global Positioning System Measurements," *Geophys. Res. Lett.*, **19**, *537-540, 1992.*.

[3] Dickey, J. O., "1 high Time Resolution Measurements of Earth Rotation," in *Advances in Space Research*, Pergamon, in press, 1994.

[4] Lichten, S. M., and J. S. Border, "Strategies for High-Precision Global Positioning System Orbit Determination," *J. Geophys. Res.*, 92, 12751-12762, 1987.

[5] Lichten, S. M., "Estimation and Filtering for High-Precision GPS Positioning Applications," *Man. Geod.*, **15**, 159-176, 1990.

[6] Yoder, C. F., J. G. Williams, and M. E. Parke, "Tidal Variations of Earth Rotation," *J. Geophys. Res.*, 86, 881-891, 1981.

[7] Gross, R. S., "The Effect of Ocean Tides on the Earth's Rotation as Predicted by the Results of an Ocean Tide Model," *Geophys. Res. Lett.*, 20,293296, 1993.

[8] Herring, T. A., and D. Dong, "Measurement of Diurnal and Semidiurnal Rotation Variations and Tidal Parameters of the Earth," *J. Geophys. Res.*, submitted, 1993.

[9] Seiler, U., "Periodic Changes of the Angular Momentum Budget Due to the Tides of the World Ocean," *J. Geophys. Res.*, 96, 10,2?87- 10,300, 1991.